Extended explanation of Q.Clear reconstruction

Q.Clear uses a block sequential regularized expectation maximization (BSREM) method for reconstruction. It includes a point-spread function (PSF) modeling and controls the noise through the use of a penalty term[1]. The penalty term imposes more smoothing in lower activity regions and less smoothing in higher activity regions, resulting in smoother cold backgrounds and improved hot lesion signal-to-noise ratios. At the same time, the use of the penalty function allows an effective SUV convergence, providing more accurate values[2–4].

The behavior of Q.Clear is controlled by a parameter β, included in the following penalty functions:

$$\Phi(x) = \sum_i y_i \log([Px]_i + r_i) - ([Px]_i + r_i) - \beta R(x) \quad (1)$$

$$R(x) = \sum_j \sum_{k \in N_j} w_{jk} \sqrt{\beta_j \beta_k} \frac{(x_j - x_k)^2}{x_j + x_k + \gamma |x_j - x_k|} \quad (2)$$

The parameter γ controls the importance of the relative difference of pixels, to avoid an oversmoothing, principally on the image edges[5], although the unique possible user input parameter is the β.

1 S. Ahn and J.A. Fessler, "Globally convergent image reconstruction for emission tomography using relaxed ordered subsets algorithms," IEEE Trans Med Imaging. **22**(5), 613–626 (2003).

2 S. Ahn *et al.*, "Quantitative comparison of OSEM and penalized likelihood image reconstruction using relative difference penalties for clinical PET," Phys Med Biol. **60**(15), 5733–5751 (2015).

3 J. Nuyts and J.A. Fessler, "A penalized-likelihood image reconstruction method for emission tomography, compared to postsmoothed maximum-likelihood with matched spatial resolution," IEEE Trans Med Imaging. **22**(9), 1042–1052 (2003).

4 N. Parvizi, J.M. Franklin, D.R. McGowan, E.J. Teoh, K.M. Bradley, and F. V. Gleeson, "Does a novel penalized likelihood reconstruction of 18F-FDG PET-CT improve signal-to-background in colorectal liver metastases?" Eur J Radiol. **84**(10), 1873–1878 (2015).

5 J. Nuyts, D. Beque, P. Dupont, and L. Mortelmans, "A concave prior penalizing relative differences for maximum-a-posteriori reconstruction in emission tomography," IEEE Trans Nucl Sci. **49**(1), 56–60 (2002).

Supplemental Table 1. Image quality comparison using NEMA NU2-2012 for different reconstruction algorithms (256x256 matrix) and a lesion-to-background ratio of 2:1. Q.Clear with a β of 50, VPHD and VPHD-S using 12 subsets, 8 iterations, and a 2.0 mm gaussian filter.

Sphere diameter (cm)	Contrast Recovery (%)			Background Variability (%)		
	VPHD	VPHDS	Q.Clear	VPHD	VPHDS	Q.Clear
10	27	27	34	9.8	9.0	5.8
13	53	55	65	7.9	7.7	4.6
17	75	76	86	6.0	6.0	3.6
22	83	84	90	4.8	4.7	2.9
28	70	74	82	4.3	4.4	2.7
37	75	79	85	3.9	3.2	2.9
Lung residual (%)	-	-	-	17.3	15.9	10.3

Supplemental Table 2. Image quality comparison using NEMA NU2-2012 for different reconstruction algorithms (256x256 matrix) and a lesion-to-background ratio of 4:1. Q.Clear with a β of 50, VPHD and VPHD-S using 12 subsets, 8 iterations, and a 2.0 mm gaussian filter.

Sphere diameter (cm)	Contrast Recovery (%)			Background Variability (%)		
	VPHD	VPHDS	Q.Clear	VPHD	VPHDS	Q.Clear
10	53	56	62	9.3	8.9	8.0
13	53	63	68	7.8	7.5	6.7
17	65	76	75	6.1	6.0	5.3
22	75	79	83	4.6	4.5	4.1
28	69	70	80	3.5	3.4	3
37	74	74	84	3.1	3.1	2.9
Lung residual (%)	-	-	-	15.8	15.1	9.2

Supplemental Table 3. Image quality comparison using NEMA NU2-2012 for different reconstruction algorithms (256x256 matrix) and a lesion-to-background ratio of 8:1. Q.Clear with a β of 50, VPHD and VPHD-S using 12 subsets, 8 iterations, and a 2.0 mm gaussian filter.

Sphere diameter (cm)	Contrast Recovery (%)			Background Variability (%)		
	VPHD	VPHDS	Q.Clear	VPHD	VPHDS	Q.Clear
10	44	45	60	8.3	7.8	5.8
13	53	55	65	6.6	6.5	4.6
17	66	67	86	5.5	4.7	3.6
22	73	79	90	4.4	4.1	2.9
28	67	69	82	3.4	3.3	2.7
37	74	80	85	3.4	3.3	2.9
Lung residual (%)	-	-	-	17.1	15.8	10.3

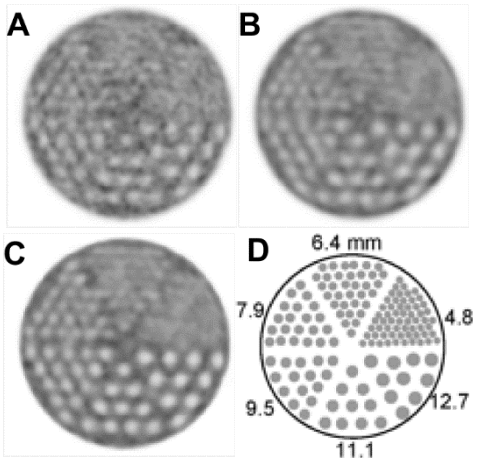

Supplemental Figure 1. Comparison of the Jaszczak phantom for the VPHD (A) ,VPHD-S (B, and Q.Clear (C) reconstructions, and (D) a cross-sectional schematic drawing of a Jaszczak phantom showing the position and diameter (in mm) of the 6 sectors of rods.

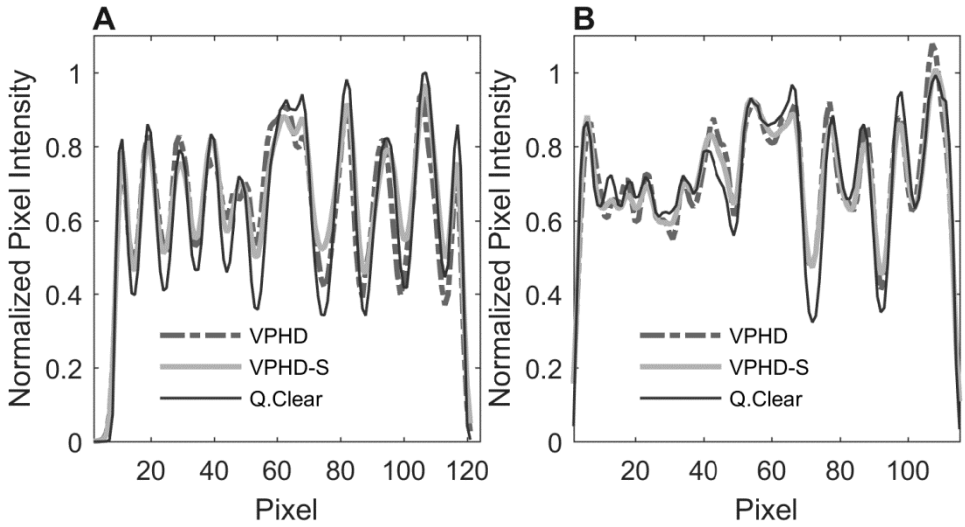

Supplemental Figure 2. Jaszczak phantom profiles: (A) horizontal across 9.5 mm and 12.7 mm rods and (B) vertical across 6.4 mm and 11.1 mm rods, for VPHD, VPHD-S, and Q.Clear reconstructions.

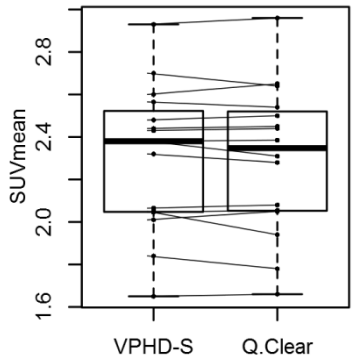

Supplemental Figure 3. Quantitative analysis of the liver VOI for VPHD-S and Q.Clear reconstructions in terms of SUV_{mean}.